

Detection and Localization of a Failure in a Pipeline Using a Kalman Filter: An Intelligent Integrated Approach Powered by Bayesian Classification

Rajamani Doraiswami and Lahouari Cheded

Abstract

An integrated approach, based on the fusion of Model-Based Approach (MBA) and Model-Free Approaches (MFA) and powered by Bayesian classification, is proposed to ensure high probability of correct estimation of leakage detection and localization with low false alarm probability to prevent disastrous consequences to the economy and environment. To ensure mathematical tractability, the nonlinear model is better approximated using linear parameter-varying (LPV) model at various operating points indicated by scheduling variables. Flows at various pipeline sections are measured and transmitted wirelessly to a monitoring station. If there is a difference in the flows across a section, it indicates a leakage, and a drone is then sent to determine the exact location of the leakage. The pipeline trajectory is accurately estimated by a human operator. Using the input and the trajectory output, termed signal, an Autonomous Kalman filter (AKF) is designed to ensure accurate tracking of the desired trajectory. The emulator-generated data are used to identify the system, complement historical data to MFA, and develop the classifier fusion. The leakage is sequentially diagnosed by judiciously selecting the most appropriate approach (MFA or MBA) to ensure a fast and accurate diagnosis. The proposed scheme was evaluated on a physical system.

Keywords: leakage diagnosis, emulators, emulator generated data, Kalman filter, sequential diagnosis, Bayes' classifier fusion, trajectory tracking, nonlinear two-tank model, linear parameter-varying model, signal model, disturbance model, measurement noise, model-based approach, model-free approach

1. Introduction

The pipelines are widely used for transporting fluids such as water or petroleum products such as fossil fuels, gases, chemicals, and other essential hydrocarbon fluids. The pipeline network covers thousands of kilometers. The effect of leak manifests as a sudden decrease in the pressure in the flow rate of fluid being transferred. Leakage in

pipes and storage tanks occurs due to factors such as faulty joints, excessive stress, aging, and holes caused by corruptions [1–10]. The leakage detection methods consist of manual inspection by trained linesmen, satellite imaging, and in recent years by autonomously guided drones flying over the pipeline route. The drone performs pipeline condition assessment and mechanical damage and cracking on above ground structures. It can be designed to detect fatigue cracking, corrosion, or other defects that cannot be observed from ground.

Classifier fusion: A Model-Based Approach (MBA) and different Model-Free schemes, lumped under the heading of Model-Free Approach (MFA) are used here. The MBA includes a Kalman filter (KF), an extended Kalman filter (EKF), an observer, and a system identification stage. For a process with an unknown model, the model-free approaches are used. In practical situations, a fusion of model-based and model-free approach; combination of the analytical and knowledge-based methods may be the most appropriate solution.

Physical system: A wider class of physical dynamic systems is nonlinear containing nonlinearities such as saturations, rate limiters, dead-zones, backlash, and turbulence. The analysis, design, estimation, identification, and control of nonlinear system are not mathematical intractable. As there is a wealth of tools for the analysis and design of linear systems, in the recent years, the Linear Parameter-Varying (LPV) systems have received a lot of attention [11, 12]. The piecewise-linear model approach helps develop computationally simple, efficient, and robust schemes for identification, design of Kalman filter, fault detection, and isolation. The LPV paradigm has become a standard formalism in systems and control, for analysis, synthesis of controllers, and even system identification.

The output of the system is a sum of signal, disturbance, and measurement noise. A signal is the desired waveform while the disturbance and the measurement noise are termed as “noise.” Wind gusts, pressure variations, and fluctuations in the flow affect the system output and are all treated as system disturbances whose effects are to be mitigated at least [2–8]. It is assumed that the stochastic disturbance and measurement noise are zero mean Gaussian processes, and that the signal, disturbance, and measurement noise are mutually uncorrelated with each other.

The principle states output will track desired trajectory *if and only if* the structure of a controller contains a) an internal model of the desired trajectory driven by the tracking error between the output and desired trajectory, and b) the closed loop system formed of the plant and the internal model is asymptotically stable.

The internal model principle governs the structure of the Kalman filter, which state that the residual is a zero mean white noise process *if and only if* the Kalman filter is a copy of the system model and driven by the residual, which the error between the output and its KF estimate. The optimality and robustness of the KF estimates are two important features of our proposed integrated approach which are both discussed in detail in [13].

1.1 Kalman filter and its properties

The KF forms the backbone of the proposed detection and localization scheme in view of its key properties [12–18].

Internal model structure: The principle states output will track desired trajectory *if and only if* the structure of a controller contains a) an internal model of the desired trajectory driven by the tracking error between the output and desired trajectory, and

b) the closed loop system formed of the plant and the internal model is asymptotically stable.

The internal model principle governs the structure of the Kalman filter, which states that the residual is a zero mean white noise process *if and only* if the Kalman filter is a copy of the system model and driven by the residual, which is the error between the output and its KF estimate. The optimality and robustness of the KF estimates are two important features of our proposed integrated approach, which are both discussed in detail in [13].

1.2 Identification using the residual of the KF

The fundamental requirement of identification is that the leftover from identification, namely the residual, is a zero-mean white noise process that contains no information. To meet this requirement, the following model-matching property of the Kalman filter

- The identified model is accurate *if and only if* the KF residual is a zero mean white noise process

Hence, the residual of model of the KF associated with the system is identified. The order of the identified model is determined from the minimal order that ensures that the identification error is a zero mean white noise process. Further there is no need for an a priori knowledge of the variance of the disturbance and measurement noise avoiding thereby solution of Riccati equation.

In model-based, model-free, and classifier fusion approach, it is crucial to provide representative and sufficient data covering the normal, perturbed, and fault-bearing operating scenarios resulting from the variations of the subsystems. As the parameters' subsystems are generally inaccessible, the data are generated indirectly by performing several off-line experiments to mimic likely operating scenarios. In model-based scheme, the emulator-generated data are used in identification of the system and the associated Kalman filter to ensure that identified models are robust to model perturbation and are significantly more accurate compared with that obtained using the classical approach of using merely the input and the output without including the perturbed models [13, 14].

The model-free approaches include Limit Checking, Visual, and Plausibility (LVP) analysis, Artificial Neural Network (ANN), Fuzzy Logic (FL), and Adaptive Neuro-Fuzzy Inference System. (ANFIS) [13–15]. The model-based approach using Kalman filtering is widely used for fault diagnosis [4, 6, 10, 12–18]. The model-free approach can readily learn the distinguishing features that help classify the system as either normal or abnormal and then isolate the faulty subsystem. However, these model-free approaches suffer from some disadvantages. For ANN, there is a lack of transparency, a need for a long-, and rich-enough training data covering most, if not all, operational scenarios, and a possibly lengthy training time. Although more transparent than ANNs, FL techniques face the problem of expressing the knowledge in the form of “if-and then” rules from the vast amount of data and from the experts' knowledge and experience. For more accuracy, the number of these rules can increase to an unacceptably large number. To overcome this problem, a combination of ANN and FL, termed ANFIS, has been proposed in recent years. However, the problem of detecting incipient faults, their fault size, and predicting the occurrence of a fault using these model-free approaches remains an unsolved and important

challenge. On the other hand, the model-based method could detect and isolate incipient faults as the model captures the complete behavior of the static and the dynamic behaviors of the system. The model predicts the behavior of the system as well as unforeseen operating scenarios, including total failure, with good accuracy. However, the behavior of a physical system at all operating points, especially the nonlinear ones, cannot be captured accurately in the form of a mathematical model [13].

In model-based, model-free, and classifier fusion approach, it is crucial to provide representative and sufficient data covering the normal, perturbed, and fault-bearing operating scenarios resulting from the variations of the subsystems. As the parameters' subsystems are generally inaccessible, the data are generated indirectly by performing several off-line experiments to mimic likely operating scenarios. In model-based scheme, the emulator-generated data are used in identification of the system and the associated Kalman filter to ensure that identified models are robust to model-perturbation and are significantly more accurate compared with that obtained using the classical approach of using merely the input and the output without including the perturbed models.

The model-free approaches include limit checking, visual, and plausibility analysis (LVP), artificial neural network (ANN), fuzzy logic (FL), and adaptive neuro-fuzzy inference system (ANFIS) [14, 15].

Practical systems are notoriously known to be complex and nonlinear in nature and hence do not lend themselves to mathematically tractable identification, analysis, and design techniques that span the entire operating region. This difficulty is further exacerbated for highly nonlinear systems. This therefore renders the use of the MBA schemes to capture both the static and dynamic behaviors of the system, difficult to use directly on the original system. On the other hand, the MFA schemes, by virtue of their independence of, and hence non-reliance on, a system model, can be readily used to learn the distinguishing features that help classify the system as either normal or abnormal and then isolate the faulty subsystem. However, these model-free approaches suffer from some disadvantages. For ANN, there is a lack of transparency, a need for a long- and rich-enough training data covering most, if not all, operational scenarios, and a possibly lengthy training time. Although more transparent than ANNs,

Fuzzy Logic (FL) techniques face the problem of expressing the knowledge in the form of "if-and then" rules from the vast amount of data and from the experts' knowledge and experience. For more accuracy, the number of these rules can increase to an unacceptably large number. To overcome this problem, a combination of ANN and FL, termed ANFIS, has been proposed in recent years.

However, the problem of detecting incipient faults, their fault size, and predicting the occurrence of a fault using these model-free approaches remains an unsolved and important challenge. On the other hand, the model-based method could detect and isolate incipient faults as the model captures the complete behavior of the static and the dynamic behaviors of the system. The model predicts the behavior of the system as well as unforeseen operating scenarios, including total failure, with good accuracy [10–13]. However, the behavior of a physical system at all operating points, especially the nonlinear ones, cannot be captured accurately in the form of a mathematical model.

The decision of the hypotheses from different classifiers is fused with a view to improving the probability of correct decision with low false alarm probability compared with that obtained by using any one of the classifiers [14]. In the proposed combined approach, the critical information about the presence or absence of a fault is gained in the shortest possible time via the faster model-free schemes such as the LVP.

A more accurate and detailed status of the subsystems is unfolded sequentially by the slower model-based scheme. The combined classifier scheme then fuses the decisions from both approaches, using a Bayes' weighted fusion method [19].

Autonomous Kalman filter: The pipeline is generally laid underground to transmit fluid flow from the source to destination over a very long distance. A trained human operator tracks the trajectory of the pipeline. It is difficult and time-consuming job to track the pipeline trajectory. A Kalman filter is designed using the input and output of the human operator. It is autonomous and replaces human operator and drives the drone accurately, efficiently, and quickly. When a leak is detected in a pipeline section, the drone is sent to the section to detect and locate the exact location from pipeline condition assessment, mechanical damage, and cracking. It can be designed to detect fatigue cracking, corrosion, or other defects that cannot be observed from ground [2].

1.3 Major contributions

The proposed scheme extends the conventional fault diagnosis approach to a wider class of MIMO Box-Jenkins model [13]. As this model is more general than conventional ones, such as AR, MA, and ARMA, it then has wider applications that may include models of systems such as transient flow in pressurized pipes and boiler-steam water flow. The emulator-generated data cover both normal and abnormal operating scenarios including various types of faults.

The emulator-generated data are employed in: (a) the identification of the system, the Kalman filter design, and fault isolation method in the model-based scheme, (b) in training the model-free schemes, and (c) in classifier fusion to ensure that the decisions made by both approaches are based on the same set of sufficient and representative data ensuring that all the diagnosis schemes are provided with a level playing field. In our proposed symbiotic approach, the performance of classifier fusion is significantly superior to that of using only a model-based or a model-free scheme, especially when the system such as a process control system is nonlinear. When the system is operating in the linear region, the performance of the model-based scheme is better while the model-free scheme such as ANN and ANFIS. However, the latter scheme outperforms the former one in the nonlinear operating region. The classifier fusion scheme ensures high probability of correct decision with low false alarm probability. The model-based scheme can detect incipient faults so that a proactive action such as a condition-based maintenance can be taken. Thanks to the availability of a reliable and accurate model, the emulators help predict likely operating fault scenarios.

When a leak is detected in pipeline section, the drone is driven autonomously to that section mimicking the human operator as it were ensuring timely leakage diagnosis, process safety, and environmental protection.

The paper is organized as follows: Section I gives an overview of the proposed scheme covering model-free and model-based schemes. In section 2, the two-tank nonlinear process control system is developed. The system is shown to be governed by a Box-Jenkins model and the identification of associated Kalman filter is developed. Section 3 presents the Kalman filter and its key properties. Section 4 gives details of the sequential fault diagnosis and discusses both the model-free schemes and the classifier fusion. Section 5 gives further details of the model-free schemes. Section 6 discusses only some important details of the model-based schemes as these have been amply discussed in some of referenced previous works. This section also evaluates the successful performance of the proposed scheme on a benchmark laboratory-scale process control system. Finally, section 7 gives the conclusion.

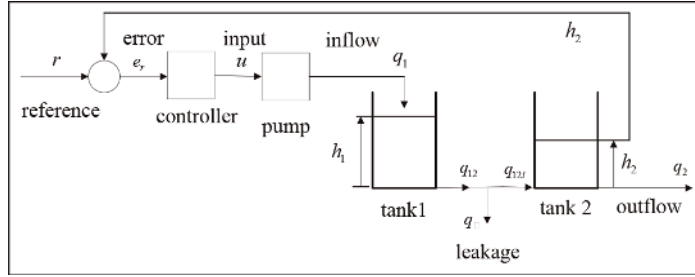


Figure 1.
Two tank process control system.

2. System model

The nonlinear model of the two-tank process control system exhibiting turbulence is approximated by piecewise linear dynamic model at each operating point using LPV approach [20]. **Figure 1** shows a two-tank process control system formed of two tanks, namely process, consumer tank denoted tank 1 and tank 2, respectively, a controller, and a pump. The controller is designed to maintain fluid level $h_2(t)$ at specified reference level $r(t)$ and is driven by the tracking error, $e_r(t) = r(t) - h_2(t)$. The control input $u(t)$ drives a pump to supply the fluid to the tank 1 and q_1 is the inflow. The fluid level of the tank 1 is $h_1(t)$. A long pipeline connects the two tanks and is subjected to a leak q_l at some section of the pipe. The outflow q_{12} of the tank 1 and q_{12l} is the inflow to the tank 2.

The tanks are cylindrical, and the height of the process tank h_1 is higher than that of the consumer tank h_2 , that is $h_1 \geq h_2$. The two tanks are connected by a long pipeline. The pressures exerted by the tank 1 and 2 at their end of the pipe are respectively $\rho g h_1$ and $\rho g h_2$, where ρ is the density of the fluid and g is the acceleration due to gravity. Since the flow is proportional to the pressure difference, fluid flows from tank 1 to tank 2. In the absence of a leak in the pipeline, the outflow q_{12} is:

$$q_{12} = \rho g (h_1(t) - h_2(t)) \quad (1)$$

In the presence of a leak, we get:

$$q_{12\ell} = \rho g (h_1(t) - h_2(t)) - q_\ell \quad (2)$$

Invoking the principle of conservation of mass, the rate of change in the volume of the tank is the difference between the inflow and outflow. Rate of change in the volume V_1 of the tank 1 is the difference between the inflow and outflow:

$$\frac{dV_1}{dt} = A_1 \frac{dh_1}{dt} = q_1 - q_{12} - q_\ell \quad (3)$$

Hence, we get:

$$A_1 \frac{dh_1}{dt} = q_1 - q_{12} - q_\ell \quad (4)$$

Where A_1 is the cross-sectional area of tank 1.

$$R_{12}(h_1 - h_2) = q_{12} \quad (5)$$

Where R_{12} is the resistance to flow between tank 1 and tank 2;
 Using (4) and (5) yields:

$$A_1 \frac{dh_1}{dt} = q_1 - R_{12}(h_1 - h_2) - q_\ell \quad (6)$$

Similarly, the rate of change in the volume V_2 of the tank 2 becomes:

$$\frac{dV_2}{dt} = A_2 \frac{dh_2}{dt} = q_{12} - q_\ell - q_2 \quad (7)$$

$$A_2 \frac{dh_2}{dt} = q_{12} - q_\ell - q_2 \quad (8)$$

Where A_2 is the cross-sectional area of tank 2, and q_2 is the outflow; As the flow is proportional to the pressure difference, we get:

$$R_2 h_2 = q_2 \quad (9)$$

Where R_2 is the resistance to outflow.

Remarks: In the laminar flow all the resistances, namely $R_{12} = \frac{d(h_1-h_2)}{dq_{12}}$ in (5) and $R_2 = \frac{dh_2}{dq_2}$ in (9) are constant as the flow is laminar. For turbulent flow, these resistances are not constant and are a nonlinear function of the height:

$$R_{12} = \frac{d(h_1-h_2)}{dq_{12}} = \xi \sqrt{h_1 - h_2}; R_2 = \frac{dh_2}{dq_2} = \xi \sqrt{h_2}; \xi \text{ is a constant}$$

Eliminating q_{12} and q_2 from the above Eqs. (7) and (8) yields:

$$A_2 \frac{dh_2}{dt} = R_{12}(h_1 - h_2) - R_2 h_2 - q_\ell \quad (10)$$

The continuous-time state space model is derived from (6) and (10), yields:

$$\begin{bmatrix} \frac{dh_1}{dt} \\ \frac{dh_2}{dt} \end{bmatrix} = \begin{bmatrix} -\frac{R_{12}}{A_1} & \frac{R_{12}}{A_1} \\ \frac{R_{12}}{A_2} & -\frac{R_2 + R_{12}}{A_2} \end{bmatrix} \begin{bmatrix} h_1 \\ h_2 \end{bmatrix} + \begin{bmatrix} \frac{1}{A_1} \\ 0 \end{bmatrix} q_1 - \begin{bmatrix} \frac{1}{A_1} \\ \frac{1}{A_2} \end{bmatrix} q_\ell \quad (11)$$

All the equations thus far including (11) are continuous. A linear discrete-time model is obtained by sampling the inputs and the outputs and the signals at uniformly spaced times as it is mathematically tractable, provided the time step is small-based, and there is a wealth of readily available and powerful analysis and design tools to use for such linearized models [21]. For example, the state-feedback controller based on the internal model principle, key properties of Kalman-filter-based system identification using residual model of KF, which for a linear system gives necessary and sufficient, whereas a nonlinear controller such as adaptive one provides only sufficient condition. Conventional approach based on observer, nonlinear filters, other nonlinear device cannot handle stochastic disturbance and measurement noise or gives only sufficient condition.

Closed-loop configuration: The MIMO system operates in a closed-loop configuration so the desired outputs to be regulated, denoted by $y_r(k)$, such as the height, track

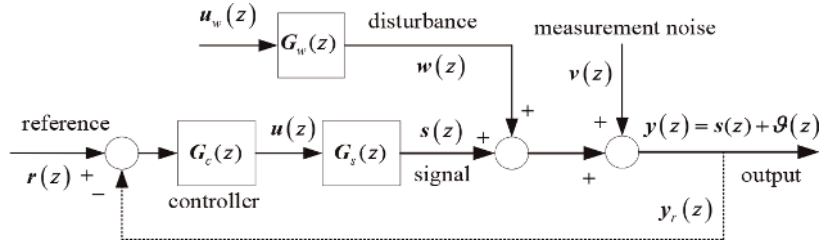


Figure 2.
Box-Jenkins model of the system relating inputs and the outputs.

the reference $y_r(k)$ as shown in **Figure 2**. The controller $G_c(z)$ is driven by the error between the reference and the output to be regulated $r(z) - y_r(z)$

$$u(z) = G_c(z)(r(z) - y_r(z)) \quad (12)$$

The signal model $G_s(z)$ is a cascade, parallel, and feedback combination of sub-systems such as the actuators, sensors, and plant.

2.1 Box-Jenkins model

Background: The Box-Jenkins method was proposed by George Box and Gwilym Jenkins in their seminal 1970 textbook *Time Series Analysis: Forecasting and Control*. The approach starts with the assumption that the process that generated the time series can be approximated using an ARMA model if it is stationary or an ARIMA model if it is nonstationary and comprises the following:

- *Model identification and model selection*
- *Parameter estimation* that best fit the selected ARIMA model. The most common methods use maximum likelihood estimation or nonlinear least-squares estimation.
- *Statistical model checking* by testing whether the estimated model conforms to the specifications of a stationary process

2.2 Box-Jenkins model of the proposed system

The augmented state-space representation of the system model, termed Box-Jenkins model (A, B, C) formed of the signal model (A_s, B_s, C_s) and disturbance model (A_w, B_w, C_w) representing a p -input, q -output system [13] is given by:

$$\begin{aligned} \mathbf{x}(k+1) &= \mathbf{A}\mathbf{x}(k) + \mathbf{B}r(k) + \mathbf{E}_w\mathbf{u}_w(k) \\ s(k) &= \mathbf{C}_s\mathbf{x}(k) \\ \mathbf{y}(k) &= \mathbf{C}\mathbf{x}(k) + \mathbf{v}(k) \end{aligned} \quad (13)$$

$\mathbf{A} = \begin{bmatrix} \mathbf{A}_s & \mathbf{0} \\ \mathbf{0} & \mathbf{A}_w \end{bmatrix}; \mathbf{B} = \begin{bmatrix} \mathbf{B}_s \\ \mathbf{0} \end{bmatrix}; \mathbf{E}_w = \begin{bmatrix} \mathbf{0} \\ \mathbf{B}_w \end{bmatrix}; \mathbf{C} = [\mathbf{C}_s \quad \mathbf{C}_w]; \mathbf{A} \in \mathbb{R}^{n \times n}$ is an augmented state-transition matrix formed of $\mathbf{A}_s \in \mathbb{R}^{n_s \times n_s}$ and $\mathbf{A}_w \in \mathbb{R}^{n_w \times n_w}; \mathbf{B} \in \mathbb{R}^{n \times p}; \mathbf{C} \in \mathbb{R}^{q \times n};$

$E_w \in \mathbb{R}^{n \times p}$ is a disturbance entry matrix; (A_s, B_s, C_s) and (A_w, B_w, C_w) are both controllable and observable. However, the signal $s(z)$ and the disturbance $w(z)$ may have spectral overlap. The Box-Jenkins model describes the system formed of the signal model, the disturbance model, their inputs, and the corrupted output.

Figure 2 shows the Box-Jenkins model representing the closed-loop system relating the reference $r(z)$, the system output $y(z)$, the output to be regulated $y_r(z)$, the controller $G_c(z)$, the signal model $G_s(z)$, input $u(z)$ to the signal model and disturbance model $G_w(z)$, disturbance $w(z)$ and the measurement noise $v(z)$.

3. Kalman filter: key properties

The KF, its residual model, and key properties are restated here for the sake of completeness and convenience of the readers [12–18]. The KF associated with the fault-free unperturbed Box-Jenkins model (A_0, B_0, C_0) given in (13) be:

$$\begin{aligned}\hat{x}(k+1) &= (A_0 - K_0 C_0) \hat{x}(k) + B_0 r(k) + K_0 y(k) \\ \hat{y}(k) &= C_0 \hat{x}(k) \\ e_{kf}(k) &= y(k) - \hat{y}(k)\end{aligned}\tag{14}$$

Where $\hat{x}(k) \in \mathbb{R}^n$ and $\hat{y}(k)$ are respectively the best estimate of the state $x(k)$, and of the output $y(k)$ of the system model (13), $e_{kf}(k)$ is the residual; the optimal Kalman gain $K_0 \in \mathbb{R}^{6n}$ ensures the asymptotic stability of the KF, i.e. $(A_0 - K_0 C_0)$; (A_0, B_0, C_0) is the identified system model embodied in the KF. The residual model of the KF relates the residual $e_{kf}(z)$ to the system, the desired target input $r(z)$, and output $y(z)$.

3.1 Key properties of the KF

The following *Lemmas* are developed here by invoking the key properties of the KF for Fault Detection and Isolation (FDI) [14]

Lemma 1:

(a) *Model-matching property*

The KF residual $e_{kf}(k)$ is a zero-mean white noise process *if and only if* the identified model of the system (A, B, C) and the true model (A_0, B_0, C_0) embodied in the KF are identical. This yields to:

$$e_{kf}(k) = e_0(k)\tag{15}$$

Where $e_0(k)$ is a zero-mean white noise process

(b) *Model-mismatch property*

If the identified model of the system (A, B, C) and the true model embodied in the KF (A_0, B_0, C_0) are not identical, then the KF residual e_{kf} will not be a zero mean white noise process. The residual will then contain an additive term $e_{kf}(k)$ termed fault indicator term, i.e.:

$$e_{kf}(k) = e_0(k) + e_{fi}(k)\tag{16}$$

The structure of the residual model of the KF, and not that of the linear regression model of the system, is such that its equation error becomes a colored noise process. The residual model is a function not only of the parameters of the system model, but also of the Kalman gain. The identification objective of ensuring that the KF residual is a zero-mean white noise process will ensure not only that the system model is accurately identified but also that the Kalman gain is optimal, thereby avoiding the need to specify the covariances of the disturbance and the measurement noise and to use the Riccati equation to solve for the optimal Kalman gain. The system model $(\mathbf{A}, \mathbf{B}, \mathbf{C})$ and its associated KF $(\mathbf{A} - \mathbf{K}\mathbf{C}, \mathbf{B}, \mathbf{C})$, are both identified without the need for the a priori knowledge of the covariances of the disturbance and the measurement noise, by minimizing the residual of the KF [12–18]:

The identified transfer functions $\frac{\bar{D}(z)}{\bar{F}(z)}$, and $\frac{\bar{N}_f(z)}{\bar{F}_f(z)}$ are used to obtain the signal model, estimates of the signal s , disturbance $w(z)$ and their associated models $(\mathbf{A}_s, \mathbf{B}_s, \mathbf{C}_s)$ are $(\mathbf{A}_w, \mathbf{B}_w, \mathbf{C}_w)$ are then derived.

Lemma 2: Signal model

The state space model of the signal model $\mathbf{G}_s(z)$ or its state space representation $(\mathbf{A}_s, \mathbf{B}_s, \mathbf{C}_s)$ relating and the signal $s(z)$, and desired target input $r(k)$ are:

$$\begin{aligned} \mathbf{x}_s(k+1) &= \mathbf{A}_s \mathbf{x}(k) + \mathbf{B}_s r(k) \\ s(k) &= \mathbf{C}_s \mathbf{x}(k) \\ \mathbf{y}(k) &= \mathbf{C} \mathbf{x}(k) - \mathbf{v}(k) \\ \hat{s}(z) &= \hat{\mathbf{G}}_s(z) \mathbf{u}(z) \end{aligned} \tag{17}$$

Where $r(k)$ is the desired target.

Lemma 3: Disturbance model

The disturbance model $\mathbf{G}_w(z)$ or its state-space representation $(\mathbf{A}_w, \mathbf{B}_w, \mathbf{C}_w)$ is derived; the KF whitens the output error $\mathfrak{d}(z) = \mathbf{y}(z) - s(z)$:

$$\begin{aligned} \mathbf{x}_w(k+1) &= \mathbf{A}_w \mathbf{x}(k) + \mathbf{B}_w u_w(k) \\ \mathbf{d}(k) &= \mathbf{C}_s \mathbf{x}_w(k) \end{aligned} \tag{18}$$

3.2 Proposed KF-based scheme

- *Lemma 1:* The fault indicator term indicates the presence or absence of fault in the system model, signal model, disturbance model, or both.
- *Lemma 2:* The presence or absence of fault in the signal model is indicated.
- *Lemma 3:* The presence or absence of fault in the signal model is indicated.

3.3 Identification: emulator generated data

In view of the key properties of the KF, it is the residual model of the KF, and not the system model, that is identified in our work, thus lending our work a novelty that sets it apart from other conventional approaches. The identification objective of

ensuring that the residual is a zero-mean white noise process will ensure not only that the system model is accurately identified but also that the Kalman gain is optimal, thereby avoiding the need to specify the covariance of the disturbance and the measurement noise and to use the Riccati equation to solve for the Kalman gain.

The system model, the signal model as well as the disturbance models are subject to perturbations. To account for these perturbations, emulators are connected in cascade to the output, the input, or both during the identification phase to mimic likely perturbations. It is shown in [13, 14] that the proposed identification scheme based on emulator parameter-perturbed experiments to generate likely model perturbations is superior to the conventional approach based on using either a conservative or an optimistic or no bound at all, instead of the true bound of the perturbed plant models.

In model-based, model-free, and classifier fusion approach, it is crucial to provide representative and sufficient data covering the normal, perturbed, and fault-bearing operating scenarios resulting from the variations of the subsystems. As the parameters subsystems are generally inaccessible, the data are generated indirectly by performing several off-line emulator-perturbed experiments to mimic likely operating scenarios.

In the model-based approach, the emulator-generated data are used in identification of the system and its associated Kalman filter to ensure that the identified models are robust to model-perturbation and are significantly more accurate compared with those obtained based on the classical approach of using merely the input and the output without including the perturbed models [13, 14]. System and the signal model and their associated KFs for the system and the signal models, estimation of the signal, disturbance are identified from the emulator-perturbed data.

The key properties of the KF are used to obtain the signal, the disturbance, and their models [14–18]. The fault-free Box-Jenkins system model (13) and the associated KF are identified the using the emulator-generated data by minimizing the residual $e_{kf}(z)$ to ensure the identified models are accurate, consistent, and reliable. Further, the emulator-generated data are used to provide data needed for the identification of the system, for the MFA, and the classifier fusion.

The identified transfer functions $\frac{D(z)}{F(z)}$, and $\frac{N_i(z)}{F_i(z)}$ are used to obtain the signal model, estimates of the signal s , disturbance $w(z)$, and their associated models (A_s, B_s, C_s) are (A_w, B_w, C_w) are derived.

3.4 State-feedback and feedforward controller

A block diagram of the feedforward-feedback controller implemented using the Kalman filter and internal model (A_{im}, B_{im}, C_{im}) is shown in **Figure 3** [20]. The system and signal models; Kalman filters associated with the system and signal models; feedback-feedforward controller; the signal s , the disturbance d , and the measurement noise v ; residual e , estimates of the signal \hat{s} and the output error $\hat{\vartheta}$ of the Kalman filter. The controller is driven by the tracking error $e_{tr}(k) = r(k) - \hat{s}(k)$.

The signal $s(z)$ instead of the noisy output $y(z)$ is employed for implementing the state feedback controller of the signal, desired trajectory, and output error

Feedforward controller: Even in the presence of model perturbations, the feedforward controller can mitigate the effect of the output error on the performance of the combined controller. The feedforward controller quickly rejects the output error without waiting for the deviation in the output to occur, hence its anticipatory

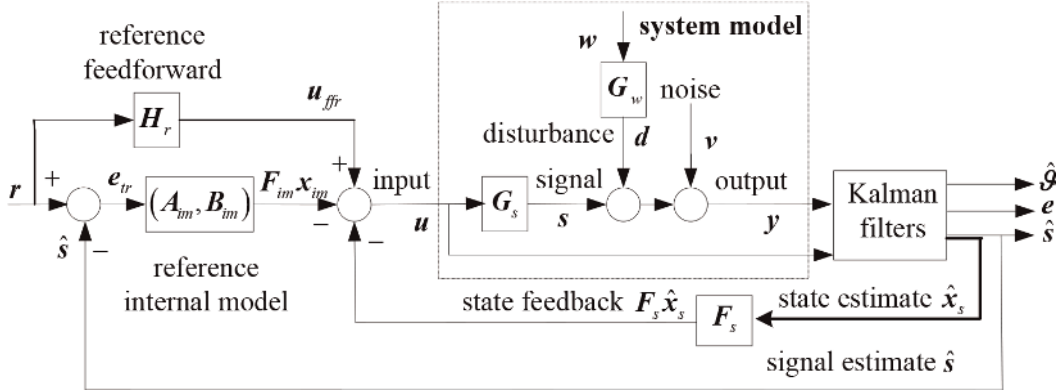


Figure 3.
Block diagram of the feedforward-feedback controller.

action. The feedforward controller of the reference, denoted by the steady-state gain H_r , is the inverse signal model evaluated at the poles of the reference model. Thus:

$$\begin{aligned} H_r &= G_s^{-1}(z) \\ u_{ffr} &= H_r r(z) \end{aligned} \quad (19)$$

3.5 Proposed Kalman filter-based scheme

The KF estimates the signal component from the output formed of an additive sum of the signal, stochastic disturbance, and measurement noise as shown.

The status of the system is asserted from the whiteness of the Kalman filter residual. A fault is detected if the residual is not a zero-mean white noise process. The faulty subsystem is isolated by estimating the perturbed emulator parameter.

When the residual is not a zero-mean white noise process signifies that either the model of the system has become faulty, i.e., a fault had occurred in the system, or the disturbance model has been perturbed, due to the purely random nature of the various disturbances affecting the system during its operation or possibly both.

3.6 Autonomous Kalman filter

Let the human operator input, u_{op} and the output y_{op} during pipeline trajectory estimation. The autonomous Kalman filter that replaces the human operator is given by:

$$\begin{aligned} \hat{\mathbf{x}}_{op}(k+1) &= (\mathbf{A}_{op} - \mathbf{K}_{op}\mathbf{C}_{op})\hat{\mathbf{x}}(k) + \mathbf{B}_{op}u_{op}(k) + \mathbf{K}_{op}y_{op}(k) \\ \hat{y}_{op}(k) &= \mathbf{C}_{op}\hat{\mathbf{x}}(k) \\ e_{op}(k) &= y_{op}(k) - \hat{y}_{op}(k) \end{aligned} \quad (20)$$

The autonomous KF drives the drone such the residual $e_{op}(k)$ is zero during entire trajectory. This will ensure that the trajectories of the human operator and KF are identical.

4. Sequential fault diagnosis

The model-free approach, namely Limit Checking and Plausibility Analysis (LCPA) and limit check, can quickly detect large faults using the limit checking, estimation of the step input responses of overshoot, rise time, and settling time. Artificial Neural Network (ANN) can capture the model of the system over both linear and nonlinear operating regimes. However, its ability to detect incipient fault critically depends upon the training data, which covers the given operating point upon the operating point, the input, and the disturbances affecting the system, the noise, and the nonlinearity effects. The same Fault Detection and Isolation (FDI) scheme may outperform other FDI schemes in some operating scenario while being outperformed by them in other scenarios. Hence, the integration of different FDI schemes will overcome this problem, in that what is missed. Relationship between these different FDI schemes will enable their collective performance to surpass that of any one of them used alone [14].

5. Model-free approaches (MFAs)

The Model-Free Approach (MFAs) are employed in monitoring the health of the system, including performance monitoring and fault detection, as it provides a macroscopic picture of the status of the system [14, 15]

5.1 Fault detection powered by the Bayesian classification for the MFA schemes

A fault in the system is asserted using Limit Checking and Plausibility (LVP) analysis from computing the step response measures of settling time, time delay, and overshoot, and using some measures based on spectral analysis, such as the frequency response and the coherence spectrum [15].

The coherence between the fault-free and actual outputs is:

$$c(y^0(\omega), y(\omega)) = \frac{|y^0(\omega)y(\omega)|^2}{|y^0(\omega)|^2|y(\omega)|^2} \quad (21)$$

Where ω is the frequency in rad/sec, and $c(y^0(\omega)y(\omega))$ are the coherence spectrum and the output of the ANN will be the fault type, i.e., either a fault in a subsystem or in a sensor. If there is no fault, then, in the ideal noise-free case, $c(y^0(\omega)y(\omega)) = 1$. Let $\hat{G}^0(\omega)$ and $\hat{G}(\omega)$ be the estimates of the frequency response of the system under normal fault-free and faulty operating regimes, respectively.

The Bayes decision strategy: The test statistic is chosen to be the median value of the coherence spectrum [14, 19]:

$$t_s = \text{median} \left\{ c \left(\hat{G}^0(\omega), \hat{G}(\omega) \right) \right\} \quad (22)$$

The Bayes decision strategy used here is given by:

$$t_s \begin{cases} \leq th & \text{for all } \omega \in \Omega \text{ nofault} \\ > th & \text{for all } \omega \in \Omega \text{ fault} \end{cases} \quad (23)$$

Where th is a threshold value, Ω is the relevant spectral region, e.g., the system bandwidth?

6. Evaluation on a physical system

The proposed sequential fault diagnosis, based on the model-based and model-free schemes, was successfully evaluated on a laboratory-scale physical process control system [7–9, 14, 15]. The controller is implemented on a two-tank process control system [22], is shown below in **Figure 4**.

6.1 Physical two-tank fluid system

The four subsystems of the two-tank system, namely the flow rate sensor γ_{s1} , the height sensor γ_{s2} , the actuator $G_1 = G_1^0 \gamma_a$ where G_1^0 is fault-free, and γ_ℓ the leakage fault indicator from the from tank 1, can be affected by either a single fault or multiple ones. As shown in **Figure 3**, when either of these fault types occurs, they are detected and isolated with the integrated approach, which intelligently processes the acquired data from the various sensors, by using the most appropriate scheme (MFA or MBA) and the Bayesian classification stage to carry out the accurate and reliable fault detection and isolation. The fault-free values are $\gamma_{si} = 1 : i = 0, 1, 2, \gamma_a = 1$ and $\gamma_\ell = 1$. The net amount of outflow is $1 - \gamma_\ell$. On the testbed used, the Lab View is used for detection and isolation of faults.

Figure 5 shows the step responses of the subsystems subject to no faults, leakage faults, actuator faults, and height sensor faults. The fault magnitudes are 0.25, 0.5, and 0.75 of the fault-free cases [14, 15]. The height, flow rate, and control input profiles under various types of faults are all shown in **Figure 5**.

Subfigures A, B, and C show respectively when there is a leakage fault, an actuator fault, and a height sensor fault. Subfigures D, E, and F show respectively the effect on the flow rate of the leakage fault, actuator fault, and sensor fault, and subfigures G, H, and I show, in the same order, the effect of these same 3 faults on the control input.

The MFA approach used here includes four essential blocks, namely a limit checks, visual and plausibility block (LVP), an adaptive neuro-fuzzy inference system block (ANFIS), a fuzzy logic block (FL), and an artificial neural network block (ANN).

Figure 5 shows the effect of disturbance, measurement noise, nonlinearity, including dead-band effect, and saturation on the actuator and on the flow rate. The unwanted effect of dead-band causes delay in the system and saturation in the actuator and flow

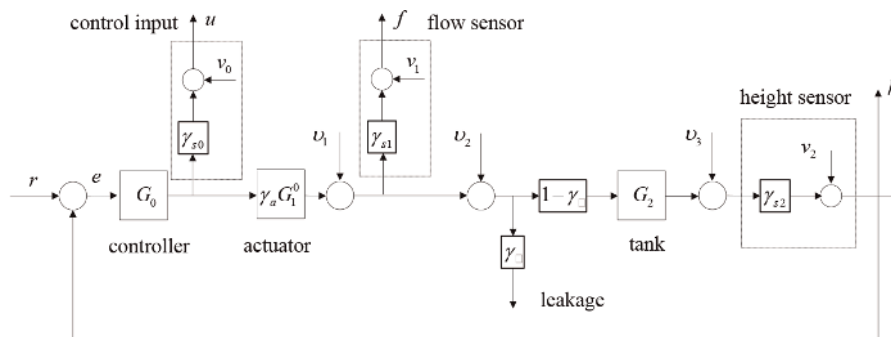


Figure 4. Process control system, with different sensors, driven by lab-view-based controller.

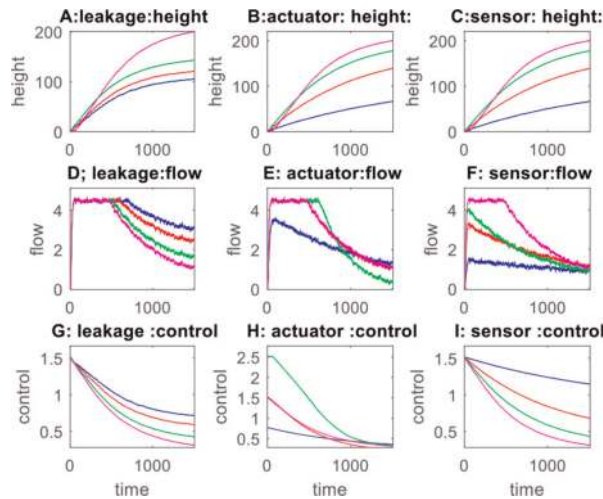


Figure 5.
 Effect of leakage, actuator, and sensor faults on height, flow rate, and control: Nonlinear case.

rate. The flow rate saturates at 4.5 ml/sec. Because of the presence of the feedback in the process system, the PI controller may reduce the effect of the nonlinearity and noise if the controller is tuned accurately. However, the PI may also dissimulate the fault by rejecting it, through its loop action, as though it were a mere disturbance. This will therefore call for a careful use of the integral action in the PI controller

6.2 Limit checking, visual, and plausibility analysis

The LPV, though limited in the size of the faults it can detect, is nevertheless the fastest of the four MFA blocks, It uses heuristics, operator experience, and the domain knowledge. It can only detect gross faults (or macro faults) but is computationally fast and monitors limit checks, flow rate, and input to the actuator for accurately determining fault status, provided the sensors are properly functioning as explained next. Some faults, such as overflow of the tanks, may not be detected or may be incorrectly reported. By way of an example, assume that the flow sensor is working properly, and the height of the tank is 250 cm, and the flow rate in the range 0 to 4 ml/sec, both of which are actual accurate values, then if the height sensor is faulty, it may then indicate an incorrect height of more than 250 cm, indicating that there is an overflow when there is none. Similarly, a faulty height sensor could report an incorrect value of 250 cm, thus indicating that the tank has reached its maximum capacity and that the sensor flow needs to be regulated to avoid an overflow, when the tank has not yet reached its full capacity. This demonstrates the weakness of the qualitative measurement of the LPV block, which, the proposed intelligent integrated approach compensates for by resorting to more accurate means of assessing the true status of the system, either through more powerful MFA blocks or through the powerful KF-based MBA block.

6.3 Artificial neural network (ANN)

ANN is a universal approximator. The height, flow rate, and control input data under leakage, actuator, and sensor faults are presented to the ANN. **Figure 4** shows

the training data formed of the height, flow rate, and control input under leakage, actuator, and sensor faults, as well as the classification of the fault types.

Remarks: Except for a very few misclassifications probably due to an insufficient amount of data processed by the ANN, the estimated classes were accurate. The FDI performance of the ANN depends crucially upon the set of input-output data employed during the training phase. The training data should be sufficient in quantity and representative enough to cover all fault-free and faulty operating regimes. In practice, it is very difficult to cover all fault scenarios, especially the extreme cases involving disasters, for which data are either scarce or unavailable. The ANN approach suffers from the lack of transparency as the decision-making process is deeply embedded in the inner workings of the ANN, thus making the rationale behind the decisions taken rather unclear to the user. Nevertheless, the ANN is computationally fast and provides timely FDI [14, 15].

6.4 Fuzzy logic approach (ANFIS)

In the case of ANN and the model-based FDI scheme, the dynamic response (covering both transient and steady-state regions) of the system is presented. However, in the fuzzy logic-based approach, only the steady-state response under various operating regimes captures the benefits of both in a single framework. As such, it is regarded as a universal approximator, where the required set of fuzzy IF–THEN rules is developed automatically from the data presented to it [14, 15].

6.5 Model-based approach

The physical two-tank fluid system is nonlinear with dead-band nonlinearity. The system was identified using the emulator-based accurate and reliable scheme proposed in [13–17] wherein several offline experiments on the physical system are performed by varying the emulator parameters to reliably capture their influence on the input-output behavior. The process control system is a closed-loop single-input and multiple-output (SIMO) system relating the input $r(k)$ to the outputs, namely the control input $u(k)$, the flow rate $f(k)$, and the height $h(k)$. The system and the associated Kalman filter are identified using the prediction error method [18]. Since multiple outputs are measured, multiple Kalman filters are employed to detect and isolate the height sensor, the flow sensor, the actuator, and the leakage faults. The multiple Kalman filters included here are associated with (a) overall closed-loop system relating the input $r(k)$, to all the outputs $u(k)$, $f(k)$ and $h(k)$, (b) $u(k)$ and $f(k)$, and (c) $f(k)$ and $h(k)$.

6.6 Bayesian hypothesis testing

Fault detection is posed as a binary composite hypothesis-testing problem [7–13, 19]. The criterion to choose between the two hypotheses, namely the presence or absence of a fault, is based on minimizing the Bayes risk, which quantifies the costs associated with correct and incorrect decisions. The $N \times 1$ Kalman filter residual data $e(k)$ are employed for this purpose. The decision between the two hypotheses is based on comparing the likelihood ratio, which is the ratio of the conditional probabilities under the two hypotheses, to a user-defined threshold value:

$$t_s(\mathbf{e}) \begin{cases} \leq \eta_{th} & \text{nofault} \\ > \eta_{th} & \text{fault} \end{cases} \quad (24)$$

Where $t_s(\mathbf{e})$ a test statistic is computed using the residual $\mathbf{e}(k)$. The test statistics $t_s(\mathbf{e})$ depends upon the class of reference input and η_{th} is some threshold value chosen to meet the stringent and conflicting requirements of a high probability of correct fault detection and isolation with low false alarm probability.

Figure 6 shows the residuals and their test statistics, and **Figure 7** shows the autocorrelations of the residuals when the system is subject to leakage, actuator, and sensor faults of various degrees such a small, medium, and large fault sizes. Subfigures A, B, and C; D, E, and F; and G, H, and I of **Figure 7** shows the residuals and their statistics when there is a leakage, actuator, and sensor faults, respectively. The test statistic is a constant bias of the residual, which is non-zero mean random process, and serves as an additive fault indicator term. The three sets of three subfigures each shown in **Figure 7** namely (A, B, and C), (D, E, and F) and (G, H, and I) show the corresponding autocorrelations for different fault types.

Remarks: The test statistics indicates the fault size associated with small, medium, and large faults.

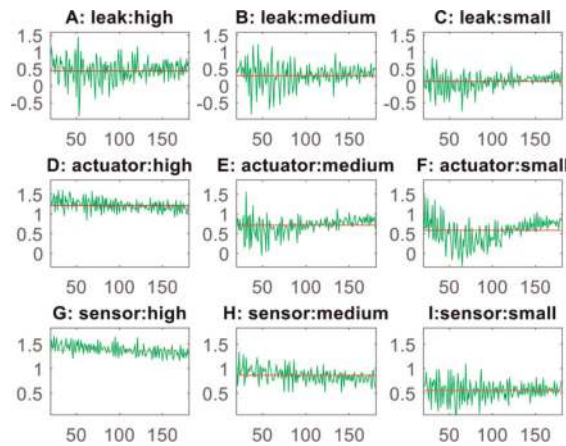


Figure 6.
 The residuals and test statistics.

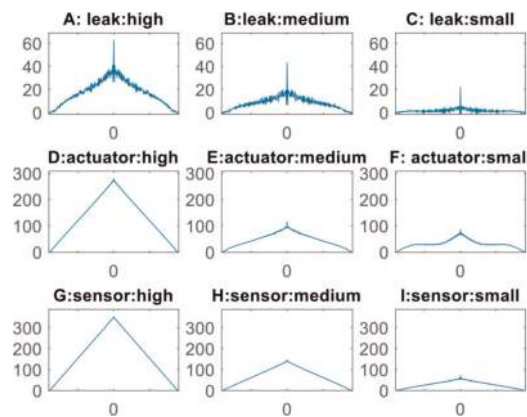


Figure 7.
 Autocorrelations of the residuals.

The Bayes decision strategy was employed to assert the fault type, i.e., to decide whether it is either leakage or actuator or sensor fault, respectively, using the fault isolation scheme proposed in [13–17]. The variance of the residual, which is the maximum value of the autocorrelation function evaluated at the origin (zero delay), indicates the fault size.

7. Illustrative example

Equivalent mathematical simulation scheme with the KF and residual (purely noise) analysis should be presented, as well as numerical data (for KF tuning, including Q and R matrices). The covariances Q and R were Q=0.1 and R=1.

The estimation of the signal, the output corrupted by disturbance and measurement noise, the spectra of the signal and the disturbance is illustrated in the following simulated example [20]. The state-space model is:

$$\begin{aligned}
 \mathbf{A}_s &= \begin{bmatrix} 0 & -0.7 & 0 & 0 \\ 1 & 1.5 & 0 & 0 \\ 0 & 0 & 0 & -0.8 \\ 0 & 0 & 1.7 & 0 \end{bmatrix}; & \mathbf{A}_w &= \begin{bmatrix} 0.3960 & -0.8025 & 0 & 0 \\ 1 & 0 & 0 & 0 \\ 0 & 0 & 1.1326 & -0.49 \\ 0 & 0 & 1 & 0 \end{bmatrix}; \\
 \mathbf{B}_s &= \begin{bmatrix} 0.5 & 1 \\ 1 & 0 \\ 1 & -0.3 \\ 0 & 1 \end{bmatrix}; & \mathbf{B}_w &= \begin{bmatrix} 1 & 0 \\ 0 & 0 \\ 0 & 1 \\ 0 & 0 \end{bmatrix}; \\
 \mathbf{C} &= \begin{bmatrix} 0 & 1 & 0 & 0 & 1.4160 & 0 & 0 & 0 \\ 0 & 0 & 0 & 1 & 0 & 0 & 2.9290 & 0 \end{bmatrix}
 \end{aligned} \tag{25}$$

Where the order $n = 8$; $y(k)$ is 2×1 output, $w(k)$ and $v(k)$ are 2×1 disturbance input, and measurement noise of unity covariance zero-mean white noise processes.

Subfigures A and B at the top of **Figure 8** compare the output and the signal. Subfigures C and D show the overlapping spectra of the signal and the disturbance.

Table 1 compares the true and estimated poles of the signal and disturbances models. The estimated poles are obtained from the model reduction techniques employed in the second stage of the two-stage identification scheme

From **Table 1**, it can be deduced that identified signal and disturbance model are accurate.

Remarks: These subfigures confirm the accuracy of the estimates of the signal and the output error established in *Lemmas 1, 2, and 3* in Section 3.

8. Kalman filter: key properties

Subfigures A and B, of **Figure 9**, compare the true step response of the signal and its Kalman filter estimate; subfigures C and D show the output error and its estimate.

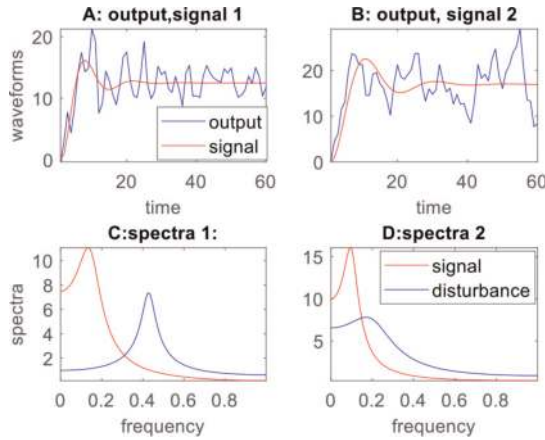


Figure 8.
 Signal and its estimate; output error and its estimate.

	True poles	Identified poles
signal $\hat{G}_s(z)$	$0.7500 \pm j0.3708$ $0.8500 \pm j0.2784$	$0.7510 \pm j0.3715$ $0.8483 \pm j0.2769$
disturbance $\hat{G}_w(z)$	$0.1980 \pm j0.8737$ $0.5663 \pm j0.4114$	$0.2031 \pm j0.8752$ <i>Identified</i>

Table 1.
 Poles of the signal and disturbance models.

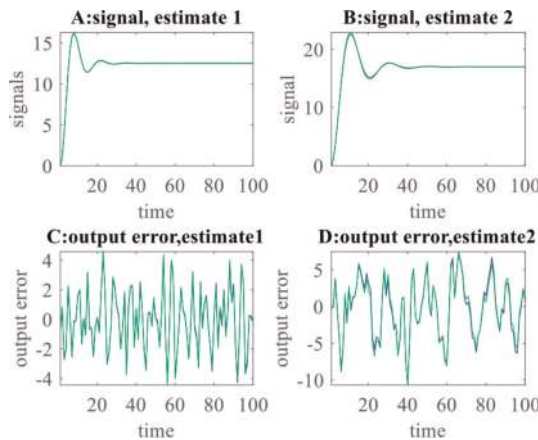


Figure 9.
 Signal and output error and their estimates.

Moreover, these subfigures clearly confirm that the equation error is a colored noise, which is whitened by the KF, thus confirming key properties of *Lemmas 1, 2, and 3*. Stated in the Section 3.

Subfigures A and B, of **Figure 10** shows the autocorrelation of the equation error, whereas subfigures C and D show the autocorrelations of the residual of the Kalman filter.

Remarks: These subfigures confirm the accuracy of the estimates of the signal and the output error established in *Lemmas 1, 2, and 3*. Confirming that the equation error

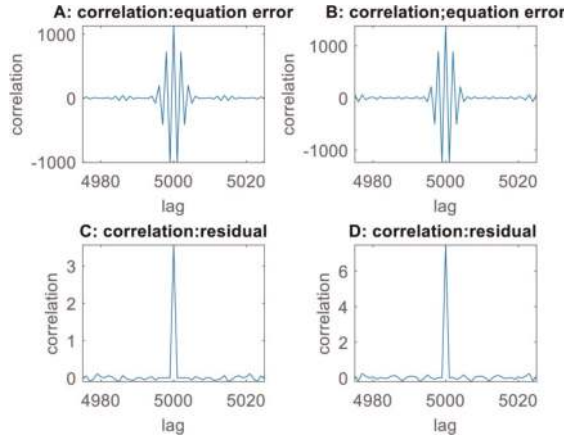


Figure 10.
Autocorrelations of KF residual and the equation error.

is a colored noise that is whitened by the KF, making the KF residual a zero-mean white noise process.

The Kalman filter-based identification of the signal and disturbance models are accurately identified the estimated poles are close to the true ones, especially those of the signal. The identification objective of ensuring the Kalman filter residual is a zero-mean white noise process will ensure not only that the system model is accurately identified but also that the Kalman gain is optimal, thereby avoiding the need to specify the covariance of the disturbance and the measurement noise and to use the Riccati equation to solve for the Kalman gain.

9. Conclusion

The novel sequential fault diagnosis approach, proposed here, is based on a judicious fusion of model-free and model-based schemes. This scheme is shown here to be superior to using (a) only the model-based scheme, (b) only the model-free scheme, or (c) the conventional combination of both schemes, in ensuring the critical requirement of a timely diagnosis and prognosis of faults with a high probability of correct decisions with a low false alarm probability. Based on extensive simulations and an evaluation on a physical system, the proposed classifier fusion scheme was shown to be reliable and efficient compared with the above-stated three conventional alternative schemes. It must be emphasized here that the novel concept of emulators and the weighted classifier scheme used here are at the core of the success of our new sequential fault diagnosis approach.

Through an integration of LPV, ANN, and FL, the model-free approach was shown to detect the presence of a possible fault quickly and reliably from the profiles of the sensor outputs. The ANN is driven by the emulator-generated data, whereas the FL is fed with steady-state values of the data. The model-free approach is also capable of providing a quick visual detection of the onset of any fault from the changes in the fault signatures such as settling time, steady-state sensor output values, and the coherence spectrum of the residuals. The fault indications obtained by the model-free approach are subsequently confirmed by the model-based approach, which, aided with a Kalman filter, provides a further necessary stage for capturing any faults, especially incipient ones, which may have escaped capture by the ANN-FL

combination due either to insufficient training data or to an incomplete set of fuzzy rules. Based on extensive simulations and an evaluation on a physical system, the proposed classifier fusion scheme was shown to be reliable and efficient compared with using only a model-based or a model-free approach alone. Thanks to the emulator-based identification, the Kalman filter was shown to be accurate, reliable, and robust to modeling uncertainties including nonlinearities and neglected fast dynamics, while retaining its sensitivity to incipient faults. Further, it can perform both diagnosis and prognosis of a fault. The model-based scheme outperforms the model-free scheme in both detection and fault isolation when the system is operating in a linear region. The ANN, if presented with sufficiently representative data, is reliable in the highly nonlinear operating region. An extension of the proposed scheme to a class of nonlinear multivariable model-based scheme is currently undergoing further analysis.

Acknowledgements

Both authors acknowledge the help in obtaining some simulation data, provided, at the early stage of this research by graduate students at The University of New Brunswick and The Office of the Vice-President (Research).

Author details


Rajamani Doraiswami^{1*} and Lahouari Cheded²

1 Department of Electrical and Computer Engineering, University of New Brunswick, Fredericton, New Brunswick, Canada

2 Life SMIEEE, UK

*Address all correspondence to: dorai@unb.ca

IntechOpen

© 2022 The Author(s). Licensee IntechOpen. This chapter is distributed under the terms of the Creative Commons Attribution License (<http://creativecommons.org/licenses/by/3.0>), which permits unrestricted use, distribution, and reproduction in any medium, provided the original work is properly cited. 

References

- [1] Datta S, Sarkar S. Review on different pipeline fault detection methods. *Science Direct Journal of Loss Prevention in the Process Industries*. 2016;**41**:97-106
- [2] Adegboye MA, Fung W-K, Karnik A. Recent advances in pipeline monitoring and oil leakage detection technologies: Principles and approaches. *Sensors*. 2019;**19**:2548
- [3] Wan J et al. Hierarchical leak detection and localization method in natural gas pipeline monitoring sensor networks. *Sensors*. 2011;**12**(1):189-214
- [4] Ziang S, Asakura T, Hayashi S. Gas leakage detection system using Kalman filter. In: 7th International Conference on Signal Processing Proceedings. IEEE Xplore. 2004;**3**:2533-2536. DOI: 10.1109/ICOSP.2004.1442297
- [5] Ferrente M, Brunone B. Pipe system diagnosis and leak detection by unsteady-state tests. *Advances in Water Resources*. Elsevier. 2003;**26**(1):95-105
- [6] An L, Sepheri N. Hydraulic actuator leak quantification using extended Kalman filter and sequential test method. In: Proceedings of American Control Conference. Minneapolis, USA: IEEE Xplore; 2006. DOI: 10.1109/ACC.2006.1657415
- [7] Zadkarami M, Shahbazian M, Salahshoor K. Pipeline leak diagnosis based on wavelet and statistical features using dempster-shafer classifier fusion technique. *Process Safety and Environmental Protection*. 2017;**105**: 156-163
- [8] Sun X, Chen T, Marquez HJ. Efficient model-based leak detection in boiler steam-water systems. *Computers and Chemical Engineering*. 2002;**26**: 1643-1647
- [9] Tang H, Yang W, Wang Z. A model-based method for leakage detection of piston pump under variable load condition. *IEEE Access*. 2019;**2019**: 99771-99781
- [10] Bensaad D, Soualhi A, Guillet F. A new leaky piston identification method in an axial piston pump based on the extended Kalman filter. *Measurement*. 2019;**148**:106921
- [11] Guest Editorial. Emerging trends in LPV-based control of intelligent automotive systems. *IET Control Theory & Applications*. 2020;**2020**:14-18
- [12] Doraiswami R, Cheded L. Linear parameter varying modelling and identification for condition-based monitoring of systems. *Journal of the Franklin Institute*. 2015;**352**(4): 1766-1790
- [13] Doraiswami R, Cheded L. Novel Direct and Accurate Identification of Kalman filter for General Systems Described by a Box-Jenkins Model. London: Intech-Open; 2019. pp. 1-26
- [14] Cheded L, Doraiswami R. A novel framework for fault diagnosis with application to process safety. *Process Safety and Environmental Protection*. 2021;**154**:168-171
- [15] Haris KM, Doraiswami R, Cheded L. Fusion of Model-Based and Model-free Approaches to Leakage Diagnosis. Kuwait: IEEE; 2009
- [16] Doraiswami R, Cheded L. Robust fault-tolerant control using an accurate emulator-based identification technique.

International Journal of Control. 2017;
2017:1336-5820

[17] Doraiswami R, Cheded L. Robust Kalman filter-based least squares identification of a multivariable system. In: IET Control Theory and Applications: The Institution of Engineering and Technology. 2018;12(8). DOI: 10.1049/iet-cta.2017.0829. Available on: www.ietdl.org

[18] Doraiswami R, Cheded L. Fault tolerance in nonlinear systems: A model-based approach with a robust soft sensor design. IET Control Theory & Applications. 2021;15(4):499-511. DOI: 10.1049/cth2.12032. Available from: <https://ietresearch.onlinelibrary.wiley.com/toc/17518652/2021/15/4> wileyonlinelibrary.com/iet-cth 499

[19] Fenton NE, Neil M. Risk Assessment and Decision Analysis with Bayesian Networks. USA: CRC Press; 2013

[20] Doraiswami R, Cheded L, Rajan S. Accurate target tracking: A New Kalman Filter Residue-based Approach Applied to a Nonlinear Multivariable Control System. In: Proceedings of the 8th International Conference of Control Systems, and Robotics (CDSR'21). Virtual Conference. May 23-25, 2021, Paper No. 303 DOI: 10.11159/cdsr21.303

[21] Proakis JG, Manolakis DG. Digital Signal Processing: Principles, Algorithms and Applications. Upper Saddle River, New Jersey: Prentice Hall; 1996

[22] Swarda K, Walvekar A, Thorat A, Mahindrakar SK. Mathematical modeling of two tank system. IJARIE-ISSN. 2017;3(2):2395-4396